



**CHALMERS**  
UNIVERSITY OF TECHNOLOGY

## **Magnetic properties of ilmenite used for oxygen carrier aided combustion**

Downloaded from: <https://research.chalmers.se>, 2026-04-06 03:40 UTC

Citation for the original published paper (version of record):

Faust, R., Lamarca, I., Schaefer, A. et al (2023). Magnetic properties of ilmenite used for oxygen carrier aided combustion. *Fuel*, 340. <http://dx.doi.org/10.1016/j.fuel.2023.127593>

N.B. When citing this work, cite the original published paper.



# Magnetic properties of ilmenite used for oxygen carrier aided combustion

Robin Faust<sup>a,\*</sup>, Ignacio Lamarca<sup>a</sup>, Andreas Schaefer<sup>a</sup>, Fredrik Lind<sup>b</sup>, Pavleta Knutsson<sup>a</sup>

<sup>a</sup> Department of Chemistry and Chemical Engineering, Chalmers University of Technology, Gothenburg 412 96, Sweden

<sup>b</sup> Department of Space, Earth and Environment, Chalmers University of Technology, Gothenburg 412 96, Sweden

## ARTICLE INFO

### Keywords:

OCAC  
Ilmenite  
Magnetic separation  
Ash  
Layer formation

## ABSTRACT

Oxygen carrier aided combustion is a combustion process that utilizes oxygen carrying particles in a fluidized bed to transport oxygen from oxygen-rich to oxygen-poor regions in the reactor. A commonly used oxygen-carrying material is ilmenite ( $\text{FeTiO}_3$ ) which is a naturally occurring mineral. At higher oxygen partial pressures ilmenite can react to pseudobrookite ( $\text{Fe}_2\text{TiO}_5$ ) and thereby take up oxygen. Upon reduction of pseudobrookite in oxygen-lean locations the oxygen is released, which enhances the distribution of oxygen through the reactor.

Ilmenite was used as bed material in an industrial 115 MW<sub>th</sub> circulating fluidized bed (CFB) boiler where recycled waste wood and wood chips were utilized as fuel. Bottom ash samples were extracted after one and two weeks and the samples were separated into two fractions by a magnetic separator. The magnetic fraction was expected to be enriched in iron-containing oxides and was therefore aimed to be recirculated into the boiler.

The SEM-EDS analysis revealed that the non-magnetic fraction consists to the largest extent of feldspar ( $\text{KAlSi}_3\text{O}_8$ ) particles. A significant amount of freshly introduced ilmenite particles was also classified as non-magnetic by the magnetic separator. Characteristic for these particles was a lack of ash layer, suggesting they had only recently been added to the system. In the magnetic fraction, several feldspar particles were found which were covered by a layer rich in Ca, Fe, Ti, and Si. Comparing the XRD analysis of the ash prior to magnetic separation with its magnetic fraction revealed a decrease of the peaks corresponding to feldspar. The removal of feldspar particles by magnetic separation was further corroborated by XRF analysis, where the concentration of K, Al and Si was significantly higher in the non-magnetic fraction, however, no changes were observed in the concentration of Fe. The present analyses shows that prolonged exposure time of ilmenite increases its magnetic susceptibility. Non-magnetic feldspar was shown to acquire significant magnetic susceptibility by formation of a surface layer containing Fe-rich attrition products from ilmenite.

## 1. Introduction

The application of biogenic resources as a replacement for fossil fuels for energy generation by thermal conversion, offers a possibility to decrease the anthropogenic CO<sub>2</sub> emissions which is a necessary step to limit climate change [1]. However, the inherent complexity of biogenic fuels necessitates the application of a suitable technology for their thermal conversion. Fluidized bed conversion (FBC) is a process that utilizes sand-like mineral particles fluidized by a gas stream which increases the heat distribution throughout the reactor [2,3]. Because of its comparably low price, quartz ( $\text{SiO}_2$ ) sand is usually used as a material in the FBC process. Despite fulfilling its function as heat carrier, quartz is inactive towards oxygen distribution which can lead to the formation of regions in the reactor which are oxygen-rich (near the gas inlet) or oxygen-poor (near the fuel inlet) which diminishes the process'

efficiency. This problem can be alleviated by the application of oxygen carriers, together or instead of the quartz sand, which are minerals that can undergo oxidation in the oxygen-rich regions of the reactor (air inlet) and reduction in the oxygen-poor ones (fuel inlet). Due to the oxygen transport provided by the oxygen carriers, less additional air needs to be added to the process to achieve optimal combustion conditions [4].

The fluidized bed combustion process utilizing an oxygen carrier is called oxygen carrier aided combustion (OCAC). The particles that are present in the reactor are prone to degrade during prolonged exposure because of attrition and ash layer build-up and therefore need to be replaced on a regular basis. The necessity of regular replacement has placed ilmenite ( $\text{FeTiO}_3$ ) into the focus of several industrial applications as it represents an economic and environmentally friendly oxygen carrier. Ilmenite is a naturally occurring mineral which is mostly used for

\* Corresponding author.

E-mail address: [faust@chalmers.se](mailto:faust@chalmers.se) (R. Faust).

<https://doi.org/10.1016/j.fuel.2023.127593>

Received 5 September 2022; Received in revised form 28 December 2022; Accepted 22 January 2023

Available online 30 January 2023

0016-2361/© 2023 The Author(s). Published by Elsevier Ltd. This is an open access article under the CC BY license (<http://creativecommons.org/licenses/by/4.0/>).

pigment production. Ilmenite is interesting for OCAC, because the contained iron atom can change its oxidation state from 2+ in  $\text{FeTiO}_3$  to 3+ in  $\text{Fe}_2\text{TiO}_5$  (pseudobrookite) at high oxygen partial pressure (air inlet) and temperatures above 900 °C [5]. At lower oxygen partial pressure (fuel inlet) the iron can change its oxidation state back from 3+ to 2+ [4,6,7]. The oxygen carrying capacity of ilmenite was found to change throughout longer exposures, and an enrichment of Fe on the surface of the particles is reported in the literature when ilmenite was used in chemical looping combustion (CLC), a related FBC process [6–8]. The migration of Fe to the surface appears to be facilitated by cracks in the particles and is associated to an increase in activity of the bed material [3,8]. The reaction responsible for the oxygen carrying effect once the Fe-rich layer has formed was suggested to be the reduction of hematite ( $\text{Fe}_2\text{O}_3$ ) to magnetite ( $\text{Fe}_3\text{O}_4$ ) at low oxygen partial pressure and vice-versa at higher oxygen partial pressure [6,9] and both hematite and magnetite were found to be present in aged ilmenite [3,7].

Ilmenite particles that are used as bed material interact with biomass ash-derived species and the formation of a Ca-enriched layer on the surface of the ilmenite particles was found [3,10]. This layer is expected to decrease the oxygen carrying ability of the particles as it covers the Fe-oxide layer. Thus, further reuse of ash-covered particles would deteriorate the performance of the OCAC process. Furthermore, the Fe that accumulates on the surface of the particles is prone to attrition which could lead to an overall loss of oxygen carrying Fe from the bed particles as fines [3]. To reduce the required addition of fresh ilmenite, as well as the deposition of used bed material, magnetic separation of oxygen carrying particles from particles that are introduced with the fuel ash can be conducted. For this, the magnetic properties of Fe-rich species can be exploited to separate the solid inventory with a magnetic separator. This can be achieved with different magnetic separation devices, such as a magnetic drum which retains magnetic particles and thereby separates them from the non-magnetic fraction [11–13]. As the Fe-rich species are concentrated in the magnetic fraction, this fraction is expected to have a higher oxygen carrying capacity than the non-magnetic. Therefore, the magnetic fraction can subsequently be recycled to the OCAC process, while the rest is deposited as a waste stream. Magnetic separation was suggested by Adánez-Rubio et al. [14], for synthetic oxygen carriers using CuO as an active phase and an Fe-Mn-oxide as a magnetic support material. The authors were able to show that the magnetic properties of the oxygen carriers are retained over several oxidation and reduction cycles, which enabled their separation from biomass or coal ash [15]. Furthermore, magnetic separation is especially beneficial for ilmenite particles that have been activated during their presence in the system. The efficiency of the magnetic separation is dependent on the magnetic properties of the bed material, which are dependent on its composition. The goal of this paper is to characterise how the magnetic properties correlate with the changes in particle composition and thereby select conditions for the magnetic separation to optimize the properties of the fraction of the bed material separated by the magnet. Recirculation of this magnetic fraction can be crucial for the process as a major part of the costs can be attributed to the required fresh bed material.

## 2. Materials and methods

### 2.1. Process and material

The process is conducted in an industrial plant which has a nominal thermal capacity of 115 MW<sub>th</sub> and is normally operated with quartz sand. For the experimental campaign discussed in this paper, Norwegian rock ilmenite was utilized with a composition as shown in Table 1. The process is operated with 60 tonnes of bed material which initially was quartz sand and was replaced by ilmenite stepwise to ensure continuous operation. As fuel, a mixture of recycled waste-wood and wood chips was used. Further information about this experimental campaign can be found by Moldenhauer et al. [12] where a magnetic fraction of 70 %

**Table 1**

Composition (in atomic percent on an oxygen-free basis) of the utilized Norwegian rock ilmenite according to the supplier (Titania A/S).

Fe	Ti	Mg	Si	Al	Mn	Ca	K	Na
48.5	40.5	6.1	2.7	1.0	0.2	0.5	0.1	0.3

after 1 week and 90 % after 2 weeks was reported. The samples analysed for this study were extracted after 1 week and 2 weeks after the addition of ilmenite to the reactor was started. For the week 1 sample, the complete ash and the magnetic fraction were analysed; for the week 2 sample, the non-magnetic fraction was investigated as well.

### 2.2. Analysis methods

Bed samples were extracted after one and two weeks. To elucidate the consequences of the magnetic separator, samples were investigated before and after the separation. The magnetic susceptibility of the samples was measured with a Bartington MS2B magnetic susceptibility sensor. The analyses were done with 12 ml of each sample, and the low frequency mode (0.46 kHz) of the device was used. Because the bulk density differed between the samples, the mass specific magnetic susceptibility was calculated. The recorded values were compared to values from the literature [16,17] (pseudobrookite from [17], the other values from [16]) which are shown in Table 2.

Qualitative crystallographic information was obtained with X-ray diffraction (XRD) with a Siemens D8 diffractometer.  $\text{Cu-K}_\alpha$  radiation was used ( $\lambda = 0.15418$  nm) and approximately 0.5 g of each sample was analysed. Prior to recording the patterns, the particles were ground to a fine powder. The results were compared to the PDF4 + 2021 database.

To obtain compositional information averaged over a comparably large number of particles at the same time, X-ray fluorescence spectrometry (XRF) was conducted with a Malvern-PANalytical Axios spectrometer. Approximately 5 g of each sample were investigated. XRF was utilized in the present study to gain insight on preferential distribution of the elements in the outer shell or in the core of the particles. Note, that in this case the ash layer is considered as the outer shell, which has a thickness of around 50  $\mu\text{m}$  after one week exposure [3]. In XRF, the attenuation length (which describes the depth from which the signal of an element is collected) is dependent on the element that is investigated, where heavier elements emit higher energy X-rays which can escape from deeper within the sample. Furthermore, a lower density of the phase through which the X-rays must travel increases the attenuation length, as less matter is present to absorb the X-rays. When performing XRF measurements, a constant density of ilmenite ( $\sim 4.5$  g/cm<sup>3</sup>) was assumed providing attenuation lengths between 10 and 20  $\mu\text{m}$  for  $\text{K}_\alpha$ -lines of the most abundant elements in ilmenite and wood ash (Ca, Ti, Fe) which range between 3.69 keV and 6.4 keV. The compositional information can therefore be considered to preferentially originate from the outer shell of the particles when the particles are analysed in their original state. In comparison to that, grinding the particles prior to XRF analysis was used to acquire information of the bulk.

To further characterize morphology and composition of the particles,

**Table 2**

Mass specific magnetic susceptibility for the phases expected to form in ilmenite used as bed material during OCAC [16,17].

Mineral/Material	Mass specific magnetic susceptibility ( $10^{-6}$ m <sup>3</sup> /kg)
Iron (Fe)	276,000
Magnetite ( $\text{Fe}_3\text{O}_4$ )	390–1116
Hematite ( $\text{Fe}_2\text{O}_3$ )	0.27–1.69
Ilmenite ( $\text{FeTiO}_3$ )	1.7–2
Pseudobrookite ( $\text{Fe}_2\text{TiO}_5$ )	0.6
Alkali-feldspar [(K,Na) $\text{AlSi}_3\text{O}_8$ ]	–0.005

scanning electron microscopy (SEM) with a Phenom ProX was conducted on particle cross-sections. These were created by embedding the particles in epoxy resin and subsequent grinding and polishing with SiC paper. Imaging was conducted by utilizing the back-scattered electron (BSE) signal and compositional information was acquired with point analysis using energy-dispersive X-ray spectroscopy (EDS). The BSE contrast of the particles was utilized to group particles with similar composition. The grouping was applied to count particles on five micrographs (around 100 particles in total per sample) to obtain statistical information on relative occurrence of ash and ilmenite particles.

### 2.3. Thermodynamic equilibrium calculations

Thermodynamic equilibrium calculations were conducted using the FactSage 7.2 software [18]. The Equilib module was utilized to acquire information on the phases which are in equilibrium at the specified conditions. The compositional data was taken from SEM-EDS. The calculations were conducted assuming 850 °C and ambient pressure (101325 Pa or 1 atm). The partial pressure of oxygen was set to 0.1 atm.

## 3. Results and discussion

To follow the effect of exposure time and ash enrichment on the magnetic separation, magnetic susceptibility measurements followed by characterization of the different fractions received before and after the use of the magnetic separator were performed.

### 3.1. Magnetic susceptibility results

The magnetic susceptibility of the samples was measured to evaluate the influence of the conditions in the boiler on the magnetic characteristics of the particles. The results are shown in Fig. 1. The measured magnetic susceptibility for fresh ilmenite was around twice as high as the literature value (Table 2), which could suggest mineral inclusions with higher magnetic susceptibility. The higher value could for example be explained by the presence of magnetite which is a component of the mined rock [19]. The measured magnetic susceptibility increases throughout the experiment, by a factor of 20 from freshly introduced ilmenite until the sample collected after 1 week of exposure and further doubled from 1 week to 2 weeks. This significant increase in magnetic susceptibility requires the formation of phases higher in magnetic susceptibility than both ilmenite and pseudobrookite (see Table 2) which

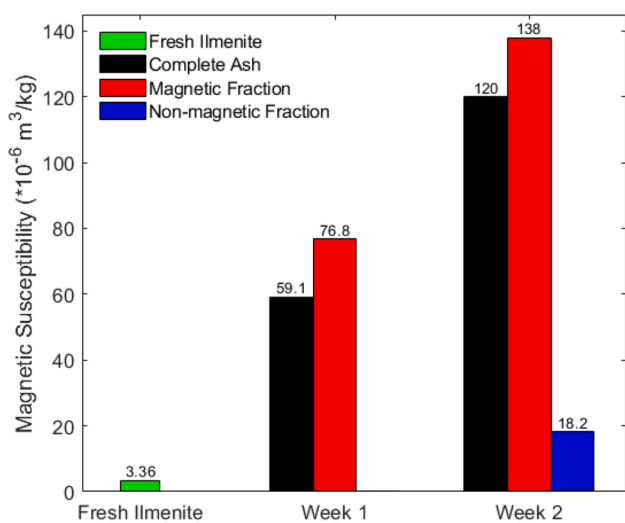


Fig. 1. Measured mass specific magnetic susceptibility of fresh ilmenite, as well as ilmenite sampled from the reactor after 1 and 2 weeks and separated by a magnet.

most likely signals that magnetite was present in the beginning and increased in share throughout the exposure. Comparing the values of the samples before and after magnetic separation, a small increase in magnetic susceptibility could be observed in the magnetic fraction. It should be noted that, even the fraction that was assigned to be the non-magnetic fraction had a magnetic susceptibility higher than fresh ilmenite, which has been found previously [12]. This confirms that fresh ilmenite that is added to the process acquires a magnetic susceptibility during prolonged residence in the process. For the magnet that was used for this study, the susceptibility of fresh ilmenite was insufficient to be classified as magnetic. Thus, based on these results, conducting the magnetic separation too early poses a risk for the fresh ilmenite to be discarded together with the non-magnetic fraction.

### 3.2. XRD results

To test the hypothesis of the development of magnetite or other more magnetic phases in the material throughout the exposure, crystallographic phase characterization of the material was performed with XRD, and the results are shown in Fig. 2. The impact of the magnetic separation can be followed by the comparison of the XRD patterns before the separation with its respective magnetic fraction. The two scans at the top of Fig. 2 depict the complete ash (black) and the magnetic fraction (red) of the sample extracted after 1 week. As expected from the magnetic susceptibilities (Table 2), the major difference between the two fractions is the lower intensity of the peaks that were assigned to feldspar ( $\text{KAlSi}_3\text{O}_8$ ) in the magnetic fraction. The same can be observed for the sample extracted after 2 weeks which is shown in the middle of Fig. 2. In both cases, the difference in peak intensity for the other phases is virtually unchanged. Similar to Corcoran et al. [3], the formation of perovskite ( $\text{CaTiO}_3$ ) was found. Perovskites are known to form solid solutions with a range of different cations, which is why an inclusion of Fe is likely [20]. However, the magnetic susceptibility of perovskite is lower than that of magnetite [21]. Over time, the development of a thicker ash layer has been observed previously on ilmenite particles [3,11]. This would mean an increase in the phases rich in ash-derived elements and thus a decrease in the overall concentration of Fe in the bed material. Comparing the week 1 samples with the week 2 samples, the intensity of the peaks corresponding to perovskite increases, which supports this concern. An increase in intensity of the peaks corresponding to magnetite ( $\text{Fe}_3\text{O}_4$ ) can be observed for the sample extracted after 2 weeks. This is in line with the previously mentioned increase in magnetic susceptibility of samples exposed for longer times and confirms the hypothesis of an increase in the magnetite fraction with time. These observations are in agreement with the results of Adánez-Rubio et al. [14] where CuO-based oxygen carriers on  $(\text{Fe,Mn})_2\text{O}_3$  support became more magnetic over time. This was attributed by the authors to the formation of more magnetic spinel  $[(\text{Fe,Mn})_3\text{O}_4]$  after several oxidation and reduction cycles.

The bottom scan shows the results of the non-magnetic fraction from week 2 of the experiment. The strongest peak was assigned to potassium-rich feldspar, however, the differentiation between anorthite ( $\text{CaAl}_2\text{Si}_2\text{O}_8$ ), albite ( $\text{NaAlSi}_3\text{O}_8$ ), and orthoclase ( $\text{KAlSi}_3\text{O}_8$ ) by means of XRD is challenging. Feldspars are the most common minerals in earth's crust and their presence in the ash fraction could be explained by contamination of the fuel, most likely the waste wood. Other major peaks correspond to pseudobrookite ( $\text{Fe}_2\text{TiO}_5$ ) and ilmenite ( $\text{FeTiO}_3$ ). The peaks corresponding to magnetite are significantly lower than in the complete ash and the magnetic fraction of week 2, albeit not absent, which explains the observed magnetic susceptibility. The relative abundance of feldspar in the non-magnetic fraction supports the efficiency of magnetic separation for reuse of oxygen carrying particles. However, the presence of Fe-rich phases such as  $\text{Fe}_2\text{TiO}_5$  and  $\text{FeTiO}_3$  suggests that even parts of the non-magnetic fraction exhibit oxygen carrying abilities and are lost in the waste streams.

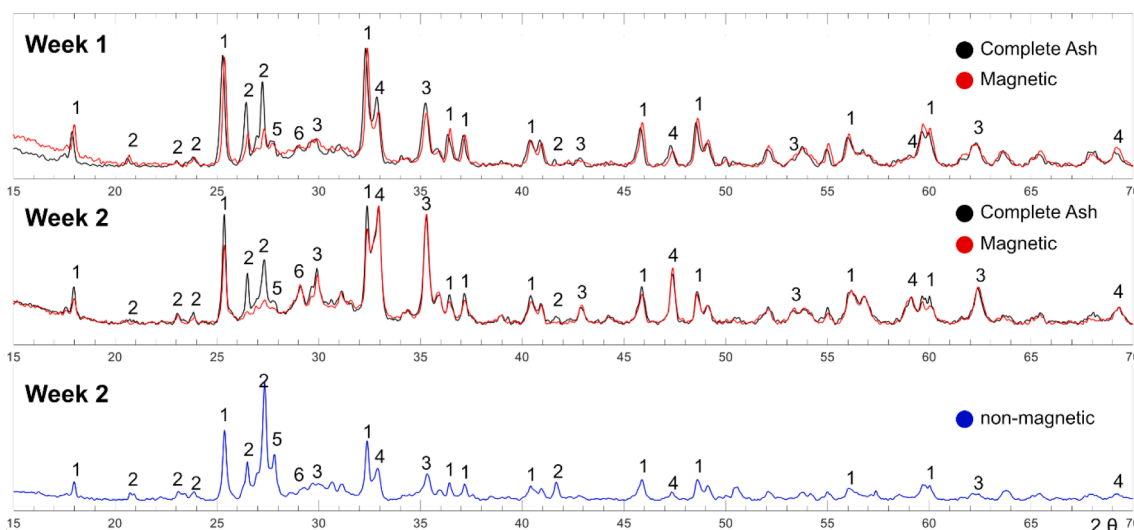


Fig. 2. Normalised XRD results. Top: complete ash (black) and magnetic fraction (red) of the sample extracted after 1 week; middle: complete ash (black) and magnetic fraction (red) of the sample extracted after 2 weeks; bottom: magnetic reject fraction (purple) extracted after 2 weeks. 1 –  $\text{Fe}_2\text{TiO}_5$ , 2 –  $\text{KAlSi}_3\text{O}_8$ , 3 –  $\text{Fe}_3\text{O}_4$ , 4 –  $\text{CaTiO}_3$ , 5 –  $\text{MgSiO}_3$ , 6 –  $\text{FeSiO}_3$ .

### 3.3. XRF results

To obtain information about the chemical composition of the samples and relate them to the crystallographic phases, XRF was conducted. The results from XRF analysis of the bed particles are shown in Fig. 3 (a). The goal of magnetic separation is to recycle the Fe from the complete ash which means its efficiency requires an increase in Fe concentration in the magnetic fraction compared to the complete ash. However, from Fig. 3 (a) it is deducible that the concentration of Fe remains nearly unchanged between the complete ash and the magnetic fraction. In the week 2 sample, the Fe concentration is even slightly lower in the magnetic fraction compared to the complete ash. While this could be caused by statistic fluctuations when selecting the sample, it is noteworthy, that no significant increase in Fe concentration in the magnetic fraction was

found. Instead, the age of the particle appears to have a greater impact on their composition, most notably in a decrease in elements inherently present in ilmenite (Fe and Ti) and an increase in elements commonly found in woody ash (Ca, Si and Mg) which is found from week 1 to week 2.

The non-magnetic fraction consists to a significant amount of Si, Al and K which are the elements found in K-feldspar ( $\text{KAlSi}_3\text{O}_8$ ). This confirms the previously discussed XRD results, where the impact of the magnetic separation was mostly found in concentrating feldspar in the non-magnetic fraction. However, XRD analysis also found  $\text{Fe}_2\text{TiO}_5$  as well as  $\text{CaTiO}_3$  which could be the crystallographic phases containing the Fe, Ti and Ca that were found with XRF. To investigate which elements are preferentially found on the outer shell compared to the bulk, the samples were investigated after being ground and the result is shown

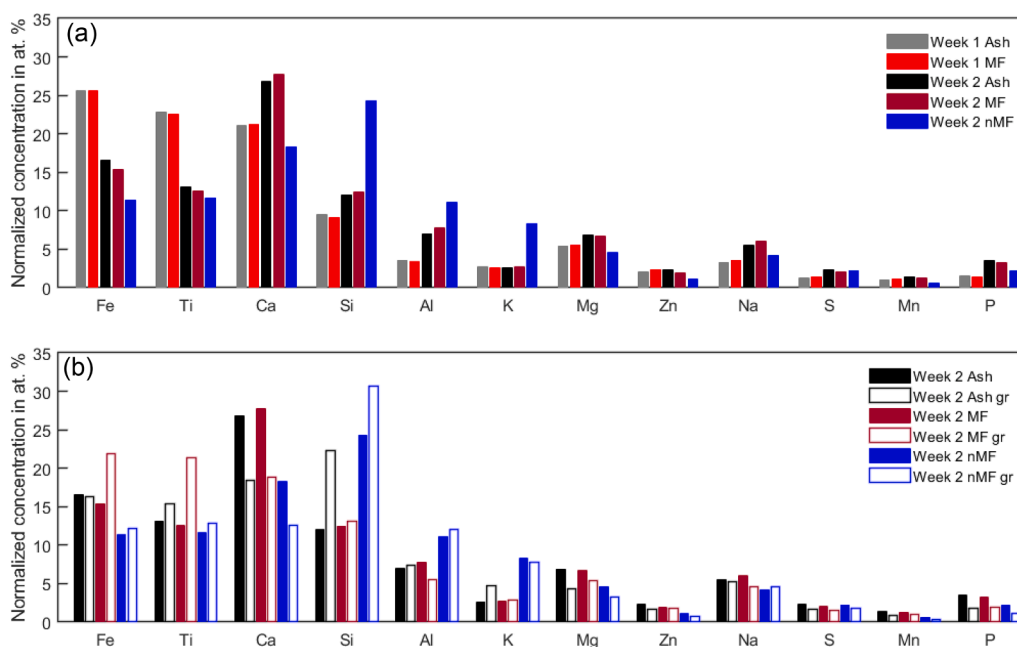


Fig. 3. XRF results showing the elemental compositions of the ilmenite bed particle samples exposed for 1 and 2 weeks (Ash) and separated in magnetic (MF) and non-magnetic fractions (nMF) (a). A comparison is made when the particles were ground (gr) to powder prior to the analysis (b). The compositions were obtained as oxides but for easier comparison with SEM-EDS, possible minor contents of carbon in the sample matrix were ignored in the analysis.

in Fig. 3 (b). The difference in concentration between the two ash fractions is most apparent in the concentration of Ca. The relative concentration of Ca is higher for both the complete ash and the magnetic fraction when the sample is not ground. This is in accordance to previously discussed Ca-distribution because Ca is expected to be deposited on the surface of the particles as it originates from the fuel ash. A similar observation can be made for Mg. The contrary is true for Fe and Ti, where the relative concentration becomes higher when the particles are ground. This observation suggests that the ilmenite particles become covered by a layer of Ca which decreases the relative concentration of Fe on the surface. However, the magnetic properties of the particles appear to remain unchanged, and they are present in the magnetic fraction after the separation. This could be detrimental for the performance of the process as a reduced concentration of Fe in surface vicinity might lead to a reduced oxygen carrying ability of the bed material.

### 3.4. SEM-EDS results

To investigate morphology and composition of individual particles and to provide further insight on the location of elements as found with XRF, SEM imaging and EDS analysis were performed. The SEM micrographs of the samples are shown in Fig. 4. Fig. 4 (a) depicts the fresh ilmenite utilized for this study. It can be seen from the contrast in the figure that the fresh material particles consist of a rather homogeneous ilmenite phase. Only one particle on the left-hand side of the micrograph contains a darker phase, which was found by EDS to have a composition corresponding to K-feldspar ( $\text{KAlSi}_3\text{O}_8$ ). The BSE signal is dependent on the average atomic number in each pixel, and a brighter contrast corresponds to a higher atomic number. It is thereby possible to differentiate between ilmenite and feldspar by the BSE contrast. Feldspar is a commonly found in the mine from which the ilmenite originates, and small amounts of this phase are therefore expected. Furthermore, the morphology of the fresh particles is rugged on the edges which is typical for particles acquired from crushing of rocks [22].

Fig. 4 (b) shows the complete ash sample extracted after 1 week of operation. From the contrast in the micrograph two types of particles can be differentiated, where some particles appear darker in contrast

and are covered by a layer of a brighter appearance. EDS analysis of these particles reveal a composition corresponding to K-feldspar ( $\text{KAlSi}_3\text{O}_8$ ). The layer that has formed on the surface of these particles is rich in Ca, Fe, and Ti, with minor amounts of Si, Mg, and Al. The particles that appear homogeneous and brighter in contrast are of a similar composition as the layers that formed around the feldspar particles. The observations made on the sample extracted after 2 weeks [Fig. 4 (c)] are similar, although the number of brighter particles in the studied sample has increased.

The impact of magnetic separation can be followed in Fig. 4 (d)–(f). The magnetic fractions of the previously discussed samples (week 1 and 2) can be seen in (e) and (f) respectively. Most of the particles appear similar in morphology and contrast to the particles which are found in the complete ash fractions. However, larger particles (similar to the ones located in the centre of both images) can be seen which have an EDS composition corresponding to ilmenite. Conversely, the non-magnetic fraction of a sample extracted after 2 weeks consists of several particles which have a composition corresponding to that of feldspar. The brighter layers that have formed on the surface are thinner than those exhibited by feldspar particles which are found in the magnetic fraction with similar exposure time [Fig. 4 (f)]. Furthermore, particles with a composition corresponding to that of ilmenite can be found in the non-magnetic fraction. This supports the previously discussed necessity of particles to remain in the process to acquire sufficient magnetic susceptibility to be identified as ‘magnetic’ by the magnetic separator. Feldspar particles which exhibit a layer containing Ca, Fe, and Ti are present in the magnetic fractions, whereas feldspar particles without this layer are in the non-magnetic fraction. Thus, the layer appears to have a greater impact on the magnetic susceptibility than the bulk material of the particle. This could be the reason why particles that are not considered as magnetic based on their composition (feldspar) end up in the magnetic fraction, once they have formed sufficiently thick layers. Indeed, the composition of the layers is similar to the content of particles that have been separated as magnetic, which supports this hypothesis.

To quantify the effect of magnetic separation, around 100 particles were counted on several micrographs of the three samples from week 2. The collected particles from each fraction were assigned to three

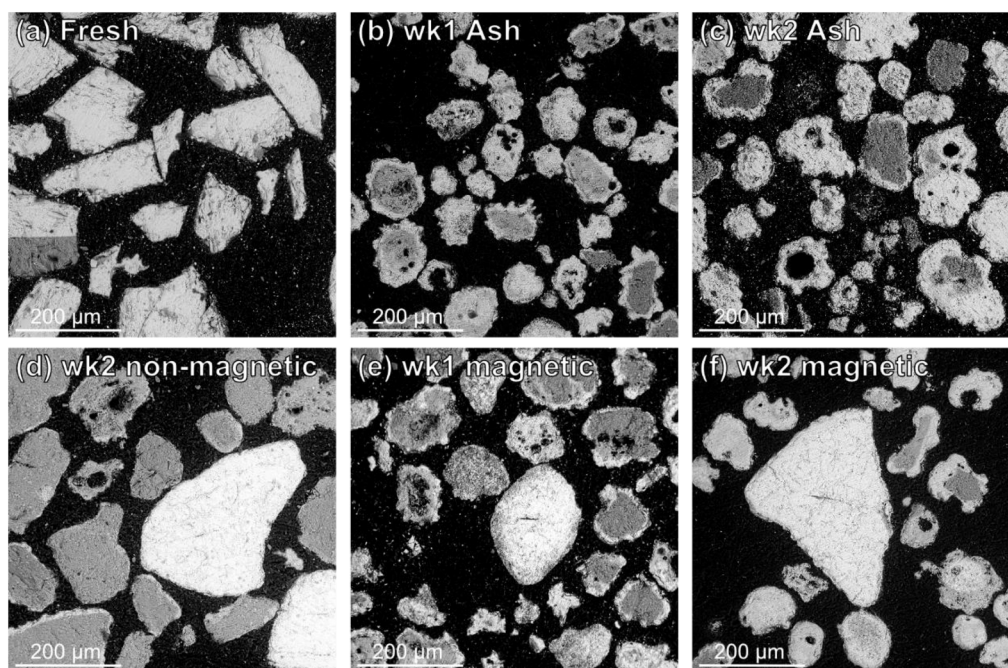


Fig. 4. SEM micrographs of cross-sections (back-scattered electron signal) of ilmenite bed material sampled after 1 and 2 weeks of exposure to combustion conditions. The images correspond to: (a) fresh ilmenite, (b) week 1 complete ash, (c) week 2 complete ash, (d) week 2 non-magnetic fraction, (e) week 1 magnetic fraction, (f) week 2 magnetic fraction.

different categories based on their major composition: ilmenite, ash, and feldspar. The results for the three fractions are shown in Fig. 5. From the figure it can be seen that the relative fractions of ash particles and feldspar particles are similar in the complete ash and the corresponding magnetic fraction. Changes in the relative amounts could possibly be assigned to statistic fluctuations, for example due to sample selection and choice of location for the micrographs. The composition of the non-magnetic fraction is significantly different, as many feldspar particles were found, but also particles with a composition corresponding to ilmenite. This agrees with the previously performed chemical analysis of the samples, which confirms that the particle selection can be considered as representative.

More than 80 % of the bed material consists of ash particles which is why their chemical composition was of special interest. The composition was measured on the magnetic fraction of the week 2 sample by EDS point analysis at the centre of cross-sections of 10 particles that were identified as ash particles according to their back-scattered electron contrast. The average composition of these particles is shown in Fig. 6. The most abundant elements found in the ash particles are Ca, Ti, Fe, and Si, of which Ca and Si are commonly found in wood ash and Fe and Ti originate most probably from the ilmenite particles. The concentrations of these elements are similar to what was previously observed with XRF on the particles which were not ground. One could therefore conclude that a phase rich in Ca, Ti, Fe, and Si is present as both ash particles and as a layer around the feldspar and ilmenite particles.

### 3.5. FactSage thermodynamic calculation results

Moldenhauer et al. [12] measured that the temperature in the furnace varied between 700 and 1000 °C, with a mean bed temperature of 850 °C. To investigate the phases which are in equilibrium in the ash particles under the conditions in the combustor, thermodynamic equilibrium calculations were conducted at different temperatures and with the average ash particle composition shown in Fig. 6. The results of the calculations are shown in Fig. 7. According to the calculations the most abundant phase found in the ash particles is CaTiO<sub>3</sub>, which agrees with the crystallographic information obtained with XRD. Furthermore, spinel was found to be thermodynamically stable phase which corresponds to a solid solution consisting mostly of magnetite (Fe<sub>3</sub>O<sub>4</sub>) that was found with XRD. The absence of pseudobrookite (Fe<sub>2</sub>TiO<sub>5</sub>) can be explained by the high concentration of Ca which leads to the formation of CaTiO<sub>3</sub> which is a thermodynamically more stable Ti-containing phase. However, pseudobrookite was found with XRD and usually forms when ilmenite is used as bed material [6–8,13]. The presence of a molten phase at temperatures above 700 °C is of special interest, as a molten phase facilitates the interaction of ash elements with the bed particles. The high concentrations of Fe and Ti in the ash particles suggest that some form of attrition has occurred which produced smaller particles which then could have been picked up by the molten phase formed on the surface of the bed particles thereby integrating the Fe and Ti.

Based on the collected results on the magnetic susceptibility and the influence of the chemical composition on it, the particles can be distinguished as dominating in ilmenite, feldspar, or as ash particles – as illustrated in Fig. 8. The figure shows schematically the development of

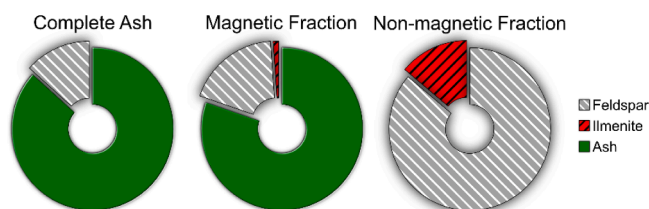


Fig. 5. Composition of particles of the three samples obtained after 2 weeks.

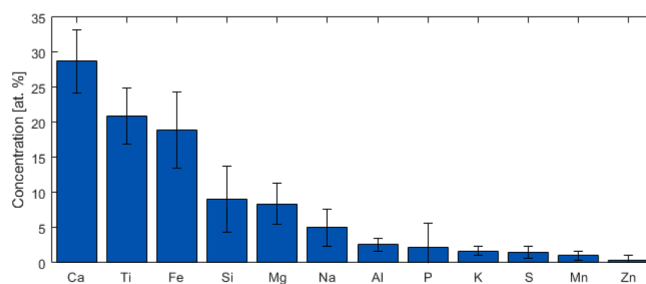


Fig. 6. Average composition of the collected ash particles based on EDS point-analysis of particles extracted on week 2 (magnetic fraction). The data is presented on an O-free basis in atomic percent.

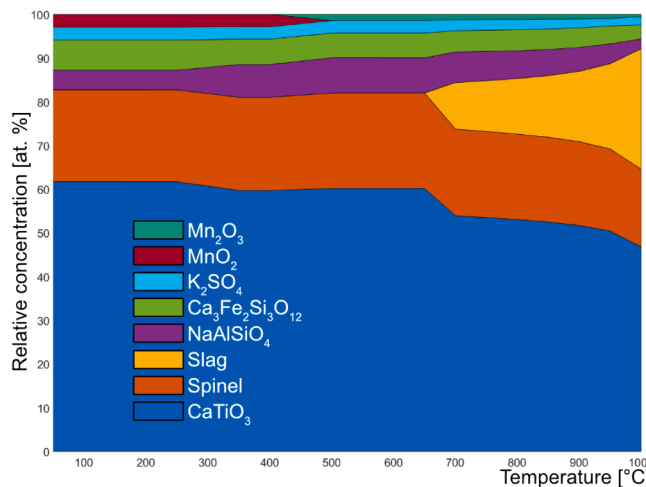


Fig. 7. Relative concentration in atomic % of phases obtained by thermodynamic equilibrium calculations with FactSage. The calculations correspond to the average composition of the ash particles (Fig. 6). The oxygen partial pressure was assumed as 0.1 atm and the total pressure as 1 atm.

the magnetic susceptibility of the different particles during the exposure.

## 4. Conclusion

Ilmenite bed material was obtained from an industrial-scale fluidized bed reactor under OCAC conditions. The properties of the magnetically separated ash fractions were investigated.

- Freshly added ilmenite is not separated by the magnet that was used in this study which can be explained by ilmenite's low initial magnetic susceptibility. Longer exposure times at high temperatures increase the magnetic susceptibility as magnetite is formed and the particles are therefore separated into the magnetic fraction by the magnetic separator.
- Fuel-ash derived elements interact with the surface of ilmenite and lead to the formation of perovskite (CaTiO<sub>3</sub>).
- Attrition of the surface of the ilmenite particles leads to the tearing off of the formed layer and the presence of Fe-rich fines in the system which can accumulate and form larger particles. These ash particles consist of elements found in ilmenite and biomass ash (Ca, Fe, Ti, Si) and make up most of the particles found in the magnetic fraction.
- Feldspar particles are introduced to the system, most likely together with the fuel. These particles exhibit low magnetic susceptibility and represent the main fraction of particles that are removed by the magnetic separation.
- Fe-rich fines can be deposited on the feldspar particles and lead to the formation of a layer with a similar composition as the ash particles.

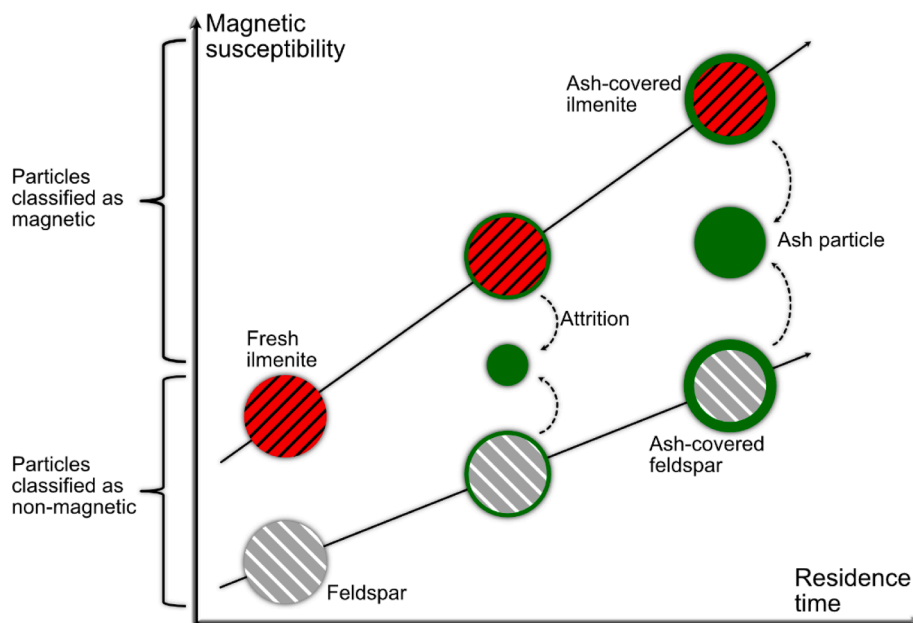


**Fig. 8.** Schematic depiction of the mechanism of development of magnetic properties of bed material particles under OCAC conditions with ilmenite used as an oxygen carrier. Three different types of particles can be distinguished as formed during combustion based on their chemical content which develop magnetic properties throughout exposure (red: ilmenite, grey: feldspar, green: ash).

Due to the Fe-content of the layer, an accumulation of a sufficiently thick layer renders the feldspar particles magnetic.

#### CRediT authorship contribution statement

**Robin Faust:** Investigation, Writing – original draft, Visualization, Methodology. **Ignacio Lamarca:** Investigation, Methodology. **Andreas Schaefer:** Investigation, Writing – review & editing, Methodology. **Fredrik Lind:** Resources, Supervision. **Pavleta Knutsson:** Conceptualization, Writing – review & editing, Supervision, Funding acquisition.

#### Declaration of Competing Interest

The authors declare that they have no known competing financial interests or personal relationships that could have appeared to influence the work reported in this paper.

#### Data availability

Data will be made available on request.

#### Acknowledgements

We would like to thank the Swedish Energy Agency project nr 50450-1 and Improb AB for financial support.

#### References

- [1] Edenhofer O, et al. The IPCC Special Report on Renewable Energy Sources and Climate Change (CC) Mitigation. Intergovernmental Panel on Climate Change 2011.
- [2] Störner F, Lind F, Rydén M. Oxygen Carrier Aided Combustion in Fluidized Bed Boilers in Sweden—Review and Future Outlook with Respect to Affordable Bed Materials. *Appl Sci* 2021;11(17):7935. <https://doi.org/10.3390/app11177935>.
- [3] Corcoran A, Knutsson P, Lind F, Thunman H. Mechanism for Migration and Layer Growth of Biomass Ash on Ilmenite Used for Oxygen Carrier Aided Combustion. *Energy Fuels* 2018;32(8):8845–56. <https://doi.org/10.1021/acs.energyfuels.8b01888>.
- [4] Thunman H, Lind F, Breitholtz C, Berguerand N, Seemann M. Using an oxygen-carrier as bed material for combustion of biomass in a 12-MWth circulating fluidized-bed boiler. *Fuel* 2013;113:300–9. <https://doi.org/10.1016/j.fuel.2013.05.073>.
- [5] Bhogeswara Rao D, Rigaud M. Kinetics of the oxidation of ilmenite. *Oxid Met* 1975; 9(1):99–116. <https://doi.org/10.1007/BF00613496>.
- [6] Adánez J, Cuadrat A, Abad A, Gayán P, de Diego LF, García-Labiano F. Ilmenite Activation during Consecutive Redox Cycles in Chemical-Looping Combustion. *Energy Fuels* 2010;24(2):1402–13. <https://doi.org/10.1021/ef900856d>.
- [7] Cuadrat A, Abad A, Adánez J, de Diego LF, García-Labiano F, Gayán P. Behavior of ilmenite as oxygen carrier in chemical-looping combustion. *Fuel Process Technol* 2012;94(1):101–12. <https://doi.org/10.1016/j.fuproc.2011.10.020>.
- [8] Knutsson P, Linderholm C. Characterization of ilmenite used as oxygen carrier in a 100 kW chemical-looping combustor for solid fuels. *Appl Energy* 2015;157: 368–73. <https://doi.org/10.1016/j.apenergy.2015.05.122>.
- [9] Larsson A, Israelsson M, Lind F, Seemann M, Thunman H. Using Ilmenite To Reduce the Tar Yield in a Dual Fluidized Bed Gasification System. *Energy Fuels* 2014;28(4):2632–44. <https://doi.org/10.1021/ef500132p>.
- [10] Corcoran A, Marinkovic J, Lind F, Thunman H, Knutsson P, Seemann M. Ash Properties of Ilmenite Used as Bed Material for Combustion of Biomass in a Circulating Fluidized Bed Boiler. *Energy Fuels* 2014;28(12):7672–9. <https://doi.org/10.1021/ef501810u>.
- [11] Gyllén A, Knutsson P, Lind F, Thunman H. Magnetic separation of ilmenite used as oxygen carrier during combustion of biomass and the effect of ash layer buildup on its activity and mechanical strength. *Fuel* 2020;269:117470. <https://doi.org/10.1016/j.fuel.2020.117470>.
- [12] Moldenhauer P, Gyllén A, Thunman H, et al. A Scale-Up Project for Operating a 115 MWth Biomass-Fired CFB boiler with Oxygen Carriers as Bed Material. 5th International Conference on Chemical Looping. Utah, USA: Park City; 2018.
- [13] Staničić I, Backman R, Cao Yu, Rydén M, Aronsson J, Mattisson T. Fate of trace elements in Oxygen Carrier Aided Combustion (OCAC) of municipal solid waste. *Fuel* 2022;311:122551.
- [14] Adánez-Rubio I, Bautista H, Izquierdo MT, Gayán P, Abad A, Adánez J. Development of a magnetic Cu-based oxygen carrier for the chemical looping with oxygen uncoupling (CLOU) process. *Fuel Process Technol* 2021;218:106836. <https://doi.org/10.1016/j.fuproc.2021.106836>.
- [15] Adánez-Rubio I, Samprón I, Izquierdo MT, Abad A, Gayán P, Adánez J. Coal and biomass combustion with CO<sub>2</sub> capture by CLOU process using a magnetic Fe-Mn-supported CuO oxygen carrier. *Fuel* 2022;314:122742. <https://doi.org/10.1016/j.fuel.2021.122742>.
- [16] Dearing JA. Environmental magnetic susceptibility: using the Bartington MS2 system. Kenilworth: Chi Pub; 1994.
- [17] Hanžel D, Sevěšek F. Characterization of Monoclinic Fe<sub>2</sub>TiO<sub>5</sub> by Mössbauer Spectroscopy and Magnetic Susceptibility. *Mat Res Bull* 1984;19(1):35–9.
- [18] Bale CW, Bélsisle E, Chartrand P, Decterov SA, Eriksson G, Gheribi AE, et al. FactSage thermochemical software and databases, 2010–2016. *Calphad* 2016;54: 35–53.
- [19] Dixon CJ, editor. *Atlas of Economic Mineral Deposits*. Dordrecht: Springer Netherlands; 1979.

- [20] Mashkina E. Structures, ionic conductivity and atomic diffusion in  $A(\text{Ti}_{1-x}\text{Fex})\text{O}_{3-\delta}$  derived perovskites (A=Ca, Sr, Ba). Friedrich-Alexander-Universität Erlangen-Nürnberg; 2005.
- [21] Chen P, Sun Y, Yang L, Xu R, Luo Y, Wang X, et al. Utilization of Metallurgy—Beneficiation Combination Strategy to Decrease  $\text{TiO}_2$  in Titanomagnetite Concentrate before Smelting. *Minerals* Dec. 2021;11(12):1419.
- [22] Mayrhuber S, Normann F, Yilmaz D, Leion H. Effect of the oxygen carrier ilmenite on NOX formation in chemical-looping combustion. *Fuel Process Technol* Nov. 2021;222:106962. <https://doi.org/10.1016/j.fuproc.2021.106962>.